Bulletin of Earthquake Engineering
https://doi.org/10.1007/s10518-022-01521-w

ORIGINAL ARTICLE

Seismic fragility assessment of bridges with as-built and retrofitted splice-deficient columns

Eyitayo A. Opabola[1] · **Sujith Mangalathu**[2]

Received: 3 February 2022 / Accepted: 16 September 2022

Abstract
A significant proportion of existing bridges in high seismic regions were constructed prior to the 1970s. As a result of poor reinforcement detailing, pre-1970s bridge columns are susceptible to lap-splice or shear failure in the plastic region. Given the high economic impact of retrofitting all pre-1970s reinforced concrete (RC) bridges, it is essential to identify the most vulnerable bridges for retrofit prioritisation. Analytical fragility functions are useful for quantifying the seismic vulnerability of existing bridge stock. However, the accuracy of these fragility functions relies on the adequacy of the adopted modelling approach. This paper presents a hinge-type modelling approach for capturing the seismic response of as-built splice-deficient and retrofitted RC bridge columns. Fragility analysis is carried out for typical seat and diaphragm abutment two-span bridges using the proposed hinge-type modelling approach. The results showed that the vulnerability of the bridges depends on the column failure mode and the limit state under consideration. Also, the common notion that the column is the most vulnerable component may not necessarily be true. The study underscored that retrofitting columns without retrofitting other components may not effectively mitigate the damage and associated risk.

Keywords Splice-controlled columns · RC bridges · Seismic fragility · Retrofitted bridge columns

1 Introduction

Damages to earthquake-prone bridges can cause significant disruptions to the transportation network of seismically active regions. Depending on the severity, these damages can pose a significant threat to the seismic resilience of a region, potentially impacting the region's emergency response and economy (Mangalathu 2017). The global engineering community has a common goal—mitigating the seismic risk of lifeline infrastructures such that they remain in service after a significant seismic event.

✉ Eyitayo A. Opabola
e.opabola@ucl.ac.uk

[1] Department of Civil, Environmental and Geomatic Engineering, University College London, London, UK

[2] Data Analytics Division, Mangalathu, Mylamkulam, Puthoor PO, Kollam, Kerala 691507, India

Published online: 08 October 2022

The earthquakes in California (e.g., The 1971 San Fernando Earthquake, 1989 Loma Prieta Earthquake, and 1994 Northridge earthquake) highlighted the structural vulnerabilities associated with pre-1970 RC bridges (Nims et al. 1989; Lee 1990; Lew 1990; Jennings 1997; Seible and Priestley 1999). In particular, most bridge columns constructed before 1970 are susceptible to shear or splice failure in the plastic hinge region. These undesirable column failure modes are associated with the sparsely-spaced transverse reinforcement and the presence of lap splices in the starter bars which extend into the footing. Due to the provided splice length, typically about $20d_b$ (Chai et al. 1991), the longitudinal reinforcement is unable to develop its full yield strength; combined with the low clamping pressure from the transverse reinforcement, splice failure in the columns may occur at significantly low drift demands (Seible et al. 1997). In certain cases where the available shear capacity of the column is low, either due to the short aspect ratio of the column or poor confinement, shear failure has been observed (Fung et al. 1971).

Given that it is not economically feasible to repair all bridges designed to non-seismic provisions, a key step toward seismic risk mitigation at the community level is the identification of the most vulnerable lifeline infrastructures for retrofit prioritisation. This process entails developing and adopting refined and efficient procedures to adequately capture the probable response of existing bridges so that reliable information on the seismic risk of a community's bridge stock can be made available to decision-makers.

A common approach to defining the seismic risk of a bridge stock is the application of bridge fragility functions which help indicate the damage probability of a bridge beyond a given limit state for various levels of ground shaking intensity. Extensive studies have been carried out on the seismic vulnerability of the bridge stocks through the generation of fragility functions [including but not limited to Banerjee and Shinozuka (2008); HAZUS-MH (2003); Huo and Zhang (2013); Mackie and Stojadinović (2001); Mangalathu (2017); Mangalathu et al. (2018); Padgett and DesRoches (2008); Ramanathan (2012); Xie et al. (2019); Zhang et al. (2019); Stefanidou and Kappos (2021); and Stefanidou et al. (2022)]. However, very few studies [e.g. Zhang et al. (2019)] have accounted for the lap-splice mode of failure in the generation of fragility curves. Zhang et al. (2019) explore the effect of corrosion on the fragility of bridges with lap-spliced columns. A shortcoming of the Zhang et al. (2019) approach is that the authors neglected experimental and field observations and assumed all columns with lap splices are splice-controlled. Likewise, the adequacy of the Zhang et al. (2019) approach was not explored with a large dataset of splice-controlled columns subjected to demands until zero resistance; hence, the performance of the Zhang et al. (2019) approach for predicting the response of older-type bridges at larger events may be uncertain.

With the availability of extensive experimental data on columns with short splices (Melek and Wallace 2004; Breña and Schlick 2007; Ghosh and Sheikh 2007; Harajli and Dagher 2008; Boys 2009), it is important to develop refined models to capture the seismic fragility of bridges with splice-deficient columns. Furthermore, for older-type bridges that have been prioritised for decision-making, it is important to understand whether retrofit measures or demolition is more appropriate. Such decisions require reliable information fragility of retrofitted bridges. It is noteworthy, however, in contrast with as-built RC components, that there are few codified provisions for modelling the hysteretic behaviour of retrofitted RC bridge components (with or without splice deficiency).

Due to the prevalence of a large number of pre-1970s box-girder and seat abutment bridges (Ramanathan 2012; Mangalathu 2017), the seismic fragility of box-girder and seat abutment bridges with splice-deficient columns is studied in this paper. This study adopts the failure-mode assessment approach developed by Opabola and Elwood (2021) for

modelling the hysteretic response of splice-deficient bridge columns. Firstly, a hinge-type modelling approach is presented for capturing the seismic behaviour of splice-deficient and retrofitted bridge columns. The proposed approach is validated using experimental data from cyclic tests of as-built and retrofitted bridge columns. Subsequently, a case study is carried out using the proposed modelling approach to investigate the seismic fragility of 15 configurations of as-built and retrofitted box-girder and seat abutment bridges. The case study demonstrates the advantage of appropriately considering the failure mode of bridge components in seismic vulnerability assessment frameworks. The failure mode-based hinge-type modelling approach is proposed for adoption in future research and engineering works.

2 Typical detailing and vulnerabilities of pre-1970 bridge stock

The bridge design philosophy in California before 1970 was to account for the seismic forces proportional to the dead weight of the structure (typically 6%) (Mangalathu 2017). Column sections are either limited to rectangular or circular without any architectural flares. Irrespective of the cross-section or geometric properties, the transverse reinforcement comprised of 12.7 mm diameter (#4 bar in the US) bar at 300 mm (12 inches) spacing. These hoops are spliced often in cover concrete rather than bending back into core concrete. Depending on the geometric properties of the bridge, the column longitudinal reinforcement varies from 1 to 3% (Mangalathu 2017). As noted by Chai et al. (1991), these reinforcement layouts are characterised by inadequate flexural strength and ductility. Also, the majority of the bridges are spliced with starter bars extending from the footing with a lap-splice length of 20 times the bar diameter. Chai et al. (1991) also pointed out that the shear strength provisions on bridges constructed before 1970s are less conservative, and actual flexural strength of columns typically exceed the shear strength of the columns. Hence the majority of failure modes are either shear- or splice-controlled.

Due to the vulnerabilities associated with columns with short splices, significant research efforts [e.g. Boys (2009); Breña and Schlick (2007); Ghosh and Sheikh (2007); Melek and Wallace (2004)] have been carried out to understand the seismic behaviour of these columns. These experimental results have shown that columns with short splices could be controlled by brittle-shear, flexure-shear, or bond-dominated (splice-controlled) responses.

3 Modelling the behaviour of bridge columns with short splices

3.1 Predicting the failure mode

Experimental results (Lynn et al. 1996; Ghosh and Sheikh 2007; Harajli and Dagher 2008; Boys 2009) have shown that columns with short splices are susceptible to brittle-shear, flexure-shear or splice-controlled mechanisms. The inelastic response of a column with short splices is failure mode-dependent (Opabola and Elwood 2021). Therefore, it is important to predict the probable failure mode prior to choosing a modelling technique. Opabola and Elwood (2021) proposed a strength-based approach for predicting the failure mode of columns with short splices. In this approach, the undegraded shear strength, the

probable flexural strength, and the flexural strength corresponding to the maximum tensile stress that can be developed in the splice (Fig. 1).

The flexural strength (V_p) is computed, assuming the longitudinal splices can achieve the tensile yield strength. The lateral strength corresponding to the maximum developable tensile stress in the splice (f_s) is computed by combining Eqs. (1) and (2). The undegraded shear strength can be computed using the Sezen and Moehle (2004) shear model [Eq. (3)]. More information on the strength-based approach can be found in Opabola and Elwood (2021).

$$l_{d,req} = \frac{0.5 f_y}{\sqrt{f'_c}} d_b, \text{MPa} \tag{1}$$

where $l_{d,req}$ is the required development length, f'_c is the concrete strength (in MPa units), d_b is the diameter of the spliced longitudinal reinforcement and f_y is the yield strength of the longitudinal reinforcement.

$$f_s = 1.25\left(\frac{l_{s,prov}}{l_{d,req}}\right)^{2/3} f_y \le f_y \tag{2}$$

where $l_{s,prov}$ is the provided splice length.

$$V_o = \frac{A_v f_{yt} d}{s} + \left(\frac{0.5\sqrt{f'_c}}{M/Vd}\sqrt{1 + \frac{N}{0.5\sqrt{f'_c} A_g}}\right) 0.8 A_g \tag{3}$$

where A_v is the transverse reinforcement ratio, f_{yt} is the yield strength of transverse reinforcement, d is the effective section depth, s is the transverse reinforcement spacing, f'_c is the concrete strength (in MPa units), M/Vd is the aspect ratio, N is axial load, A_g is the gross cross-sectional area of the column.

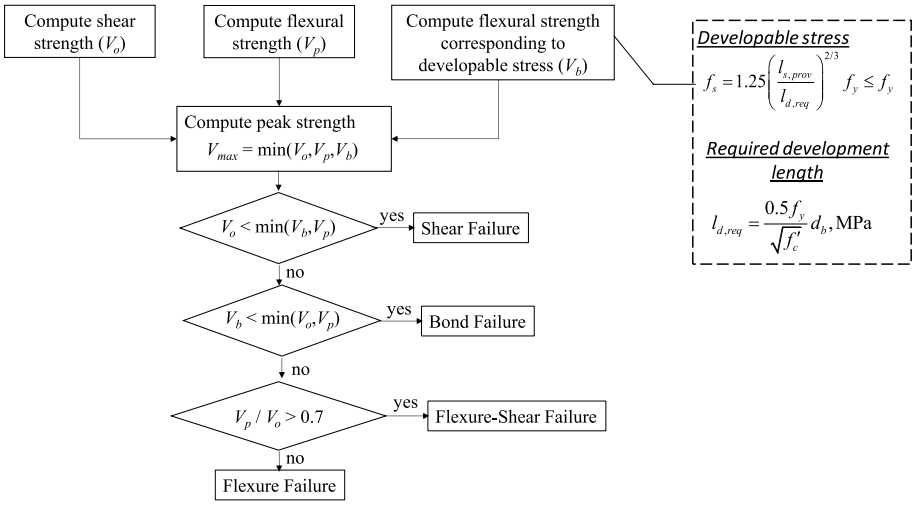

Fig. 1 Strength-based approach for predicting the failure mode of RC bridge columns

Once the failure mode of the column has been determined, the appropriate modelling approach is chosen, as presented in the subsequent subsections.

3.2 Modelling splice-controlled bridge columns

This study proposes a lumped-plasticity modelling approach for capturing the response of splice-controlled bridge columns. A lumped-plasticity model was adopted over the commonly-adopted distributed plasticity model for the following reasons:

1. Experimental data (Melek and Wallace 2004; Ghosh and Sheikh 2007) suggest that, as a result of early severe bond degradation, there is little or no stress transfer between the splices and concrete, thereby nullifying the plane section hypothesis. The rocking (fixed-end rotation) mechanism of the column can be effectively captured using nonlinear rotational springs.
2. The massive computational efforts that are required to develop reliable fragility curves with time constraints can be reduced by adopting a lumped plasticity model
3. The lumped plasticity model offers the advantage of effectively capturing cyclic strength degradation and pinching behaviour.

In the adopted approach, the bridge column model is made up of an elastic column element and zero-length nonlinear rotational springs at the end regions of the column (Fig. 2a). In this study, the modified Ibarra-Medina-Krawinkler pinching hysteretic material model (Lignos and Krawinkler 2011) was adopted for modelling the behaviour of splice-controlled columns. The column response is idealised as a trilinear moment-rotation backbone (See Fig. 2b), defined using mechanistic formulations calibrated to experimental tests on splice-controlled columns. The key backbone parameters are the elastic stiffness (K_e); the strength parameters – yield moment (M_y), maximum moment strength (M_{max}), and the residual strength capacity (M_{res}); and the deformation parameters – pre-capping rotation capacity (θ_p), post-capping rotation capacity (θ_{pc}), and ultimate rotation capacity (θ_u), and (See Fig. 2b). Also, hysteretic parameters are used to capture cyclic strength and stiffness deterioration (Λ) and pinching behaviour (κ).

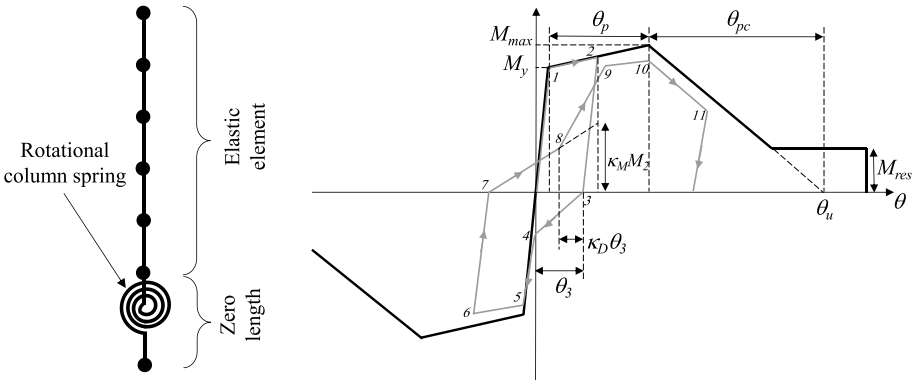

(a) hinge-type model **(b)** Moment-rotation relation

Fig. 2 Adopted hinge-type model for bridge columns

Table 1 Formulations for predicting the backbone parameters of splice-controlled columns

Parameter	Formulation	References
Elastic stiffness	$\frac{EI_{eff}}{EI_g} = \alpha\left(0.27\left(\frac{a}{d}\right) - 0.07\right) \le \alpha$	Opabola and Elwood (2020)
Pre-capping rotation capacity	$\theta_p = \lambda a_{nl,0} \le 0.03$ $a_{nl,o} = 0.75\% \le 3.9 - 0.9\frac{A_s f_s}{A_{vs} f_{yt}\left(\frac{l_{s,prov}}{s}\right)} \le 3\%$	Opabola and Elwood (2021)
Post-capping rotation capacity	$\theta_{pc} = b_{nl} - \theta_p \ge 0$ $b_{nl} = 0.1 - 0.25\frac{N}{A_g f'_c}$	Opabola et al. (2021)
Residual strength	$c = 0.2 - 0.4\frac{N}{A_g f'_c} \ge 0.0$	Opabola et al. (2021)
Stiffness deterioration (Λ)	$\Lambda = 0.4$	Opabola et al. (2021)
Pinching parameter	$\kappa = 0.6 - \frac{0.0002}{\rho_t} \ge 0.2$	Opabola et al. (2021)

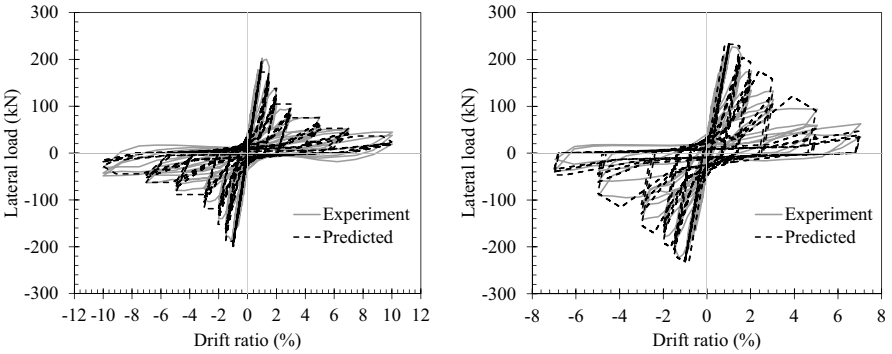

Fig. 3 Comparison of measured and predicted force–displacement response of splice-controlled bridge columns

Table 1 presents a list of formulations for predicting the backbone parameters of splice-controlled columns. The adopted formulations have been calibrated to a database of 24 splice-controlled columns with short splices [See Opabola et al. (2021) for more exhaustive analysis and inference].

where the effective stiffness coefficient from ASCE/SEI 41 (α) is the flexural rigidity coefficient from ASCE/SEI 41–17 (ASCE 2017) and taken as 0.3 for $N/A_g f'_c \le 0.1$, $\alpha = 0.7$ $N/A_g f'_c \ge 0.5$ and linear interpolation for $0.1 < N/A_g f'_c < 0.5$; a/d is the aspect ratio of the column; λ is a coefficient accounting for the influence of axial load and it is equal to 1 for $N/A_g f'_c \le 0.2$ and 0 for $N/A_g f'_c \ge 0.5$. A linear interpolation is required for $0.2 < N/A_g f'_c < 0.5$. A_v is the transverse reinforcement area, f_{yt} is the yield strength of the stirrups, s is the stirrup spacing, $l_{s,prov}$ is the provided lap splice length, A_s is the total area of longitudinal bars in the tensile face of the column section and f_s is the developable tensile stress.

A comparison of the numerical model results with the experimental results from Melek and Wallace (2004) (Fig. 3a) and Massicotte and Boucher-Proulx (2008) (Fig. 3b) is

presented in Fig. 3. As depicted in Fig. 3, the modelling approach captures the response of the column specimens up until the total degradation of lateral resistance.

3.3 Modelling flexure-shear and shear-controlled bridge columns

Studies (Elwood 2004; LeBorgne and Ghannoum 2014) have proposed limit-state materials for triggering shear failure and activating a nonlinear shear spring that controls strength and stiffness deterioration. While the Elwood (2004) approach adopts a displacement-based limit surface, LeBorgne and Ghannoum (2014) provide the flexibility of adopting a force-based and/or deformation-based limit surface, which triggers degrading behaviour when a defined deformation or force limit is attained. Axial failure can also be captured using axial limit-state materials proposed by the authors. In this study, the LeBorgne and Ghannoum (2014) approach has been adopted for modelling flexure-shear and brittle shear-controlled columns with short splices.

3.4 Modelling retrofitted bridge columns

Given the failure of bridge columns in pre-1970s bridges, over the last three decades, significant research efforts (Shinozuka et al. 2002; Kim and Shinozuka 2004; Padgett and DesRoches 2008; Billah et al. 2013) have been devoted to exploring the feasibility of improving the seismic performance of bridge columns using local retrofitting techniques—i.e. column jacketing. This section adopts observations and conclusions from existing experimental programs in adopting a modelling approach for retrofitted bridge columns.

An experimental study by Seible et al. (1997) looked at the seismic performance of steel-jacketed and FRP-jacketed bridge columns. In comparison with the as-built shear-controlled and splice-controlled bridge columns, the jacketed columns had large ductility and energy dissipation capacities. Comparing the force–displacement backbone curves of steel-jacketed and FRP-jacketed bridge columns from the Seible et al. (1997) tests, it can be concluded that the choice of retrofit technique tends to influence the effective stiffness and peak strength of the test specimens. The influence of the retrofit technique (steel vs FRP jackets) on peak strength and effective stiffness can be attributed to the fact that the column section in the steel-jacketed column is increased by the jacket-encased concrete. On the other hand, the shapes of the force–displacement backbone curves for the steel-jacketed and FRP-jacketed bridge columns suggest that the inelastic response and hysteretic behaviour of the columns may be similar.

In terms of inelastic response, experimental results show that the behaviour of jacketed splice-controlled columns is dominated by a fixed-end rotation mechanism (Harajli and Rteil 2004; Haroun and Elsanadedy 2005; Harajli and Dagher 2008). Based on data from Harajli and Dagher (2008), fixed-end rotation accounts for up to 80% of total deformation during the inelastic phase. While the dominating mechanism for both retrofitted and as-built splice-controlled columns is similar, the significantly improved confinement level in retrofitted columns enhances the concrete-rebar bond strength; thereby enabling adequate stress transfer between the splices and strain penetration over a good proportion of the column height.

The effectiveness of column jacketing as a viable low-maintenance technique has been demonstrated in past seismic events (Housner 1994). There is, however, still a gap in modelling the response of retrofitted bridge columns. Appropriate modelling techniques are desirable to predict the probable response of retrofitted bridge columns in future strong events.

Studies have adopted the distributed plasticity approach using fibre-type elements in modelling retrofitted columns. While the adopted approach in these studies can capture the enhanced ductility capacity of the columns, they do not capture the true response of the retrofitted columns. Fibre-type models are well-known to capture deformation due to flexural curvature. To capture bond-slip and shear deformations, additional inelastic springs are typically adopted. This modelling approach is more ideal for slender code-conforming columns where bond-slip deformation is typically less than 30% of total deformation. In the case of retrofitted columns where bond-slip deformation can account for 80% of total deformation, the adoption of the fibre-type model may be questionable.

Interestingly, most existing studies [e.g. Padgett and DesRoches (2008)] do not consider bond-slip deformation in the modelling approach. The authors are also unaware of studies that have demonstrated the capability of fibre-type models to capture the hysteretic response of retrofitted columns with fixed-end dominated behaviour. This might be a research gap for future studies.

In this study, the nonlinear rotational spring has been adopted for modelling retrofitted columns. The adopted approach is applicable to both steel-jacketed and FRP-jacketed bridge columns. Also, the approach overcomes the limitations of the fibre-type models by effectively capturing cyclic strength degradation without convergence problems and reducing computation time.

The increased effective stiffness of steel-jacketed columns can be accounted for by computing the equivalent moment of inertia of the retrofitted column (typically circular or elliptical). The yield (M_y) and flexural strength (M_{max}) of jacketed columns can be derived from a section analysis.

To compute the drift capacity parameters, the confinement level provided by the FRP wrapping can be converted to an equivalent amount of transverse reinforcement $A_{v,eff}$ at a given spacing s_{eff} equating the lateral confining stress from the FRP wraps to that developed by transverse reinforcement, similar to a procedure described in Alvarez and Brena

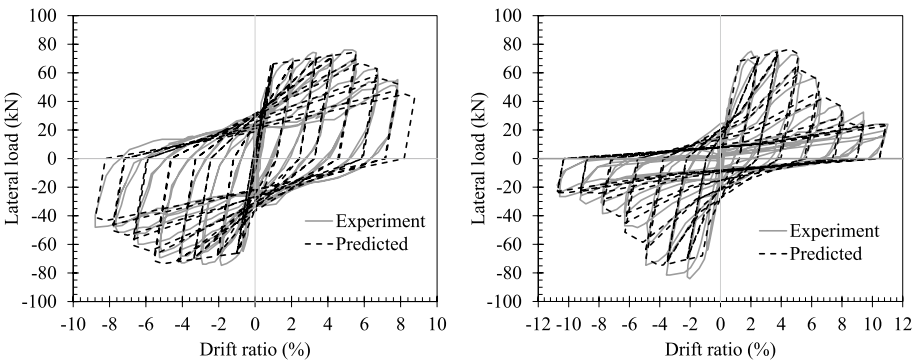

Fig. 4 Comparison of measured and predicted force–displacement response of retrofitted bridge columns

(2014). From the equivalent $A_{v,eff}$ and s_{eff}, the corresponding equivalent ratio of transverse reinforcement spacing to effective depth (s_{eff}/d) and the equivalent transverse reinforcement ratio ($\rho_{t,eff}$) can be computed. Using the computed equivalent transverse reinforcement parameters and the axial load level, the modelling parameters can be computed using formulations proposed by Haselton et al. (2016).

Figure 4 shows the adequacy of the adopted approach for FRP-retrofitted square and circular columns from an experimental test program by Ghosh and Sheikh (2007). As shown in Fig. 4, the adopted approach captures the hysteretic behaviour of the columns up to large drift demands; hence, providing confidence in the application of the proposed approach for capturing the seismic response of bridges up until collapse.

4 Case study bridges

To explore the seismic performance of as-built and retrofitted older-type bridges with lap splice in the plastic hinge region, three different cases are considered in this study: (1) bridges with splice-controlled columns; (2) bridges with flexure-shear-controlled columns; and (3) bridges with FRP-jacketed columns.

Based on the assumption that the splices do not influence the seismic response of a flexure-shear-controlled column with short splices, results from case 2 are also relevant for flexure-shear-controlled columns with continuous longitudinal reinforcement.

For the sake of appropriate comparison with as-built bridges, FRP jacketing was chosen as the retrofit technique. This is because, due to the unchanged effective stiffness of the FRP-retrofitted column, the natural period of the column remains unchanged. However, it is expected that the results presented in this study are also valid for steel-jacketed columns where there is a minor increase in cross-section relative to the as-built columns, given that the same level of ductility capacity is achievable in both FRP- and steel-jacketed columns.

As California bridge inventory comprises diaphragm and seat abutment bridges, these abutment types are considered for each case. In diaphragm abutment bridges, the deck is rigidly connected to the abutments, while the deck rests on bearings in the case of seat abutment bridges. The study is limited to two-span bridges as they occupy the major portion of California bride inventory (Mangalathu 2017). Also, different seat widths are possible for the bridges constructed before the 1970s. A nomenclature, as shown in Table 2, is defined. Such a nomenclature helps to identify the relative vulnerability of various components in the selected cases. Per the nomenclature, S-S-S4 corresponds to a bridge with a flexure-shear-controlled column (S) with seat abutments (S) with a seat width greater than 24 inches (S4). In total, 15 bridge configurations were considered.

The FRP retrofit design entailed providing confinement to ensure sufficient clamping is provided to inhibit splice failure and also improve the shear strength of the column (to preclude shear failure following flexural yielding). The FRP design was carried out using the procedure outlined in Seible et al. (1997). Carbon fibre reinforced polymer (CFRP) was employed for the purpose of this study. A modulus of elasticity of 160 GPa was assumed for the CFRP. Following the Seible et al. (1997) procedure, the required CFRP thickness was estimated as 4.7 mm.

Table 2 Nomenclature of the case study bridges

Column configuration	Abutment type	Seat with class	Possible configurations
Splice-controlled (LS) Flexure-shear-controlled (S) FRP-jacketed (FRP)	Diaphragm (D) Seat (S)	4–12 in. (S1) 12–18 in. (S2) 18–24 in. (S3) > 24 in (S4)	LS-D, S-D, FRP-D, LS-S-S1, LS-S-S2, LS-S-S3, LS-S-S4, S-S-S1, S-S-S2, S-S-S3, S-S-S4, FRP-S-S1, FRP-S-S2, FRP-S-S3, FRP-S-S4

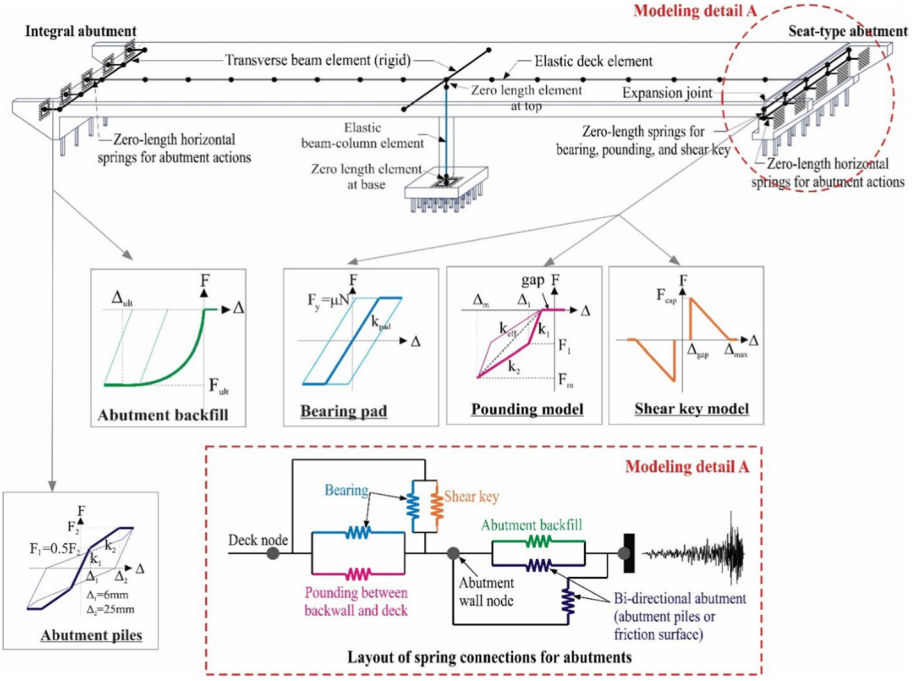

Fig. 5 Modeling of various bridge components

5 Numerical modeling and fragility analysis

Fragility curves are generated based on the cloud analysis approach and the seismic demand on the bridge components is estimated through three-dimensional nonlinear time-history analyses. The typical layout of a two-span box girder bridge is shown in Fig. 5. The Finite element modelling of the bridge is carried out with the OpenSees platform (Mazzoni et al. 2006) which can account for geometric as well as material uncertainties. As there is no damage expected to the superstructure during an earthquake, the superstructure is modelled using the elastic element with mass lumped along the centerline. As shown in Fig. 5, monolithic solid diaphragms are modelled using transverse rigid elements. The column is modelled with the linear-elastic element with two zero-length spring elements in the transverse and longitudinal axes at the bottom end and only one zero-length spring element in the transverse axis at the top end. The zero-length element properties are varied according to the bridge cases (splice-controlled, flexure-shear-controlled, FRP-jacketed), as explained in the previous section. The contact element developed by Muthukumar and DesRoches (2006), which explicitly accounts for the loss of hysteretic energy, is used to model the pounding between the decks. The Bilinear model suggested by Mangalathu et al. (2016) is used to model the bearings.

The response of the abutment in longitudinal and transverse directions is also considered in this study. The longitudinal response includes passive and active resistance. The passive resistance is provided by the backfill soil and the piles, while the active resistance and the transverse resistance are provided only by the piles. The passive response of the abutment back wall is simulated using the hyperbolic soil model proposed by Shamsabadi and Yan (2008). Trilinear

springs stemming from the recommendations of Choi (2002) are used to model the abutment piles. Nonlinear elements are used to replicate the behavior of the shear key following the recommendations of Megally et al. (2001). Zero-length elements capturing the response of the abutment backfill soil and piles are connected in parallel and are connected to the transverse deck elements in the case of diaphragm abutments. Bearing pad elements and pounding elements are also modelled with zero-length spring elements and are connected in parallel. They are connected to the transverse rigid deck elements and the abutment and pile elements for seat abutments. Column footing is assumed to be fixed in this study. Interested readers are directed to Mangalathu (2017) and Ramanathan (2012) for an in-depth discussion on the analytical modelling of various bridge components, as only a summary is given in this section. Based on the extensive plan review conducted by Mangalathu (2017), the selected bridge configurations of the current study are given in Table 3.

The suite of ground motions assembled by Baker et al. (2011) for the PEER Transportation Research Program is adopted in this study. These ground motions are specifically assembled for the seismic risk assessment of infrastructure systems in California. The peak responses of the bridge components (e.g., column drift, bearing deformations, abutment deformations) are recorded for each time history analysis. The probability that the seismic demand (D) placed on a component exceeds the associated capacity (C) conditioned on a chosen intensity measure (IM) can be assessed by the fragility curves. Spectral acceleration at 1.0 s, S_a(1.0 s), is chosen as the IM in the current study based on previous research works (Ramanathan 2012; Shafieezadeh et al. 2012). Assuming a lognormal distribution for the demand and capacity, the probability of reaching or exceeding a specified damage state for a component is estimated following the work of Cornell et al. (2002).

$$\mathrm{P}\left[D > C/\mathrm{IM}\right] = \Phi\left[\frac{\ln\left(S_d/S_c\right)}{\sqrt{\beta_{d/IM}^2 + \beta_c^2}}\right] \tag{4}$$

Table 3 Geometric and material parameters for the analytical model (Mangalathu 2017)

Parameter	Values	Parameter	Values
Span (ft)	120.07	Pile spacing of abutments (ft)	7.00
Column height (ft)	22.27	Concrete strength (ksi)	4.86
Deck width (ft)	35.00	Steel yield strength (ksi)	67.35
Number of cells in box girder	3	Abutment stiffness (kip/in)	79.99
Top flange, bottom flange, and wall thickness (in)	9.12, 7.00, 12.00	Damping (%)	0.045
Depth of the box girder (in)	79.25	Restrainer length (ft)	14.00
Column diameter (in)	60	Restrainer slack (in)	0.625
Longitudinal reinforcement ratio (%)	1.5	Number of restrainers	10
Provided splice length for splice-controlled column	$20d_b$	Coefficient of friction of bearing pad	1.0
Longitudinal reinforcement size	#11	Shear modulus of the bearing pad (ksi)	0.165
Transverse reinforcement	#4 @ 12 in	Shear key gap (in)	0.75
Abutment height (ft)	6.00	Gap b/n abutment and deck	0.750

where S_d is the median estimate of the demand as a function of the IM, S_c is the median estimate of the capacity, $\beta_{d/IM}$ is the dispersion of the demand conditioned on the IM, β_c is the dispersion of the capacity, and $\Phi(\cdot)$ is the standard normal cumulative distribution function. Probability distributions of structural demand conditioned on the IM, known as the Probabilistic Seismic demand model (PSDM) are required to evaluate Eq. (5). S_d is estimated based on the power-law recommended by (Cornell et al. 2002):

$$S_d = a(\mathrm{IM})^b \tag{5}$$

where a and b are the regression coefficients. The coefficients a and b are obtained by performing a linear regression analysis on the demand-IM pair in the log-transformed normal space. Dispersion, $\beta_{d/IM}$, is evaluated based on statistical analysis as (Eq. 6)

$$\beta_{d/\mathrm{IM}} = \sqrt{\frac{\sum_{i=1}^{N}\left(\ln d_i - \ln a(\mathrm{IM})^{\mathrm{b}}\right)^2}{N-2}} \tag{6}$$

The component fragility obtained above is integrated into the bridge fragility through the joint probabilistic seismic demand model (JSPDM), recognising the correlation between the various components following the work of Nielson and DesRoches (2007).

6 Limit states

Four limit states (slight, moderate, extensive, and complete) are considered in the study, and each limit state for a specific component is characterised by the median (S_c) and the associated dispersion (β_c). The limit states are defined based on post-earthquake traffic

Table 4 Limit state models of various bridge components

Component	Units	S_c				β_c
		Slight	Moderate	Extensive	Complete	
Column drift (COL)						
Splice-controlled column	%	0.40	1.20	4.00	7.00	0.35
Flexure-shear-controlled column	%	0.60	2.00	3.00	4.00	0.35
FRP-jacketed column	%	1.00	2.50	7.50	10.00	0.35
Abutment seat						
S1	in	0.5	1.0	2.0	3.0	0.35
S2	in	1.0	3.0	6.0	9.0	0.35
S3	in	1.0	3.0	10.0	15.0	0.35
S4	in	1.0	3.0	14.0	21.0	0.35
Passive abutment response (ABP)	in	3.0	10.0	–	–	0.35
Active abutment response (ABA)	in	1.5	4.0	–	–	0.35
Transverse abutment response (ABT)	in	1.0	4.0	–	–	0.35
Deck displacement (DEC)	in	4.0	305	–	–	0.35
Bearing displacement (BRD)	in	1.0	4.0	–	–	0.35
Joint Seal (SEAL)	In	0.75	–	–	–	0.35
Shear key	In	1.50	5.0	–	–	

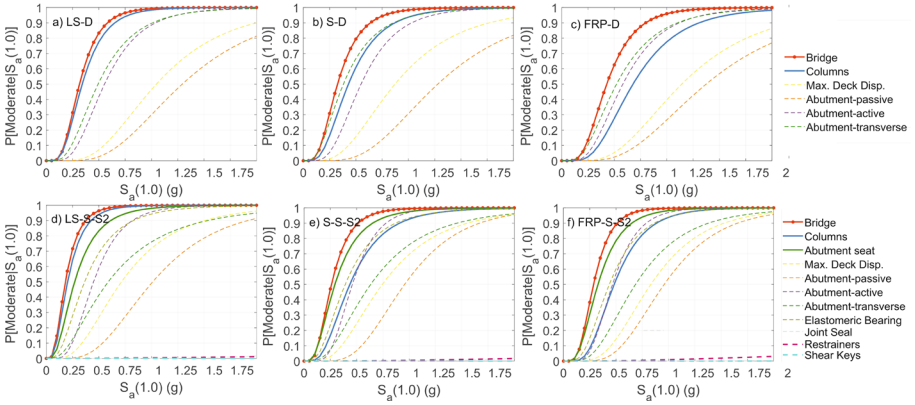

Fig. 6 System and component fragility curves for moderate damage states for various bridge configurations

Table 5 Critical components for seat abutment bridge configurations at various damage states

Column type	Damage state	Seating length			
		S1	S2	S3	S4
Splice-controlled	Slight	AS	AS	C	C
	Moderate	AS	C	C	C
	Extensive	AS	AS	C	C
	Complete	AS	AS	C	C
Flexure-shear controlled	Slight	AS	AS	AS	AS
	Moderate	AS	AS	AS	AS
	Extensive	AS	C	C	C
	Complete	AS	C	C	C
FRP-jacketed	Slight	AS	AS	AS	AS
	Moderate	AS	AS	AS	AS
	Extensive	AS	AS	AS	AS
	Complete	AS	AS	AS	AS

AS Abutment seat, *C* Column

closure and repair implications and the bridge inspection priorities (Mangalathu 2017). Another key contribution of the present study is the drift-based limit-state values for the splice-controlled, flexure-shear-controlled and FRP-jacketed bridge columns. The limit state values are given in Table 4. The values for the flexure-shear-controlled and splice-controlled columns are based on observed performance from test specimens. The limit states for the columns are defined in terms of drifts because local engineering demand parameters such as curvature ductility are mainly appropriate in components expected to be dominated by flexural curvature. For the retrofitted column, the values adopted by Mangalathu et al. (2018) for code-conforming bridge columns were chosen. This follows the experimental evidence that the performances of equivalent code conforming columns and jacketed older-type columns are similar [See Harajli and Dagher (2008)].

7 Fragility functions

Fragility functions provide a more comprehensive understanding of the relative vulnerability of the considered bridge configurations. The methodology presented in the previous section is used to develop the system and component fragility functions for the considered bridges. Typical fragility curves for the various bridge configurations are shown in Fig. 6. Table 5 summarises the critical components for the considered seat abutment bridge configurations at various damage states. In this study, the critical component is defined as the component with the least median fragility estimate. As shown in Table 5, the critical component is either the abutment seat or the column. It is, however, noteworthy that in certain cases the median fragility estimate of the seat abutment and column are relatively close (See Fig. 7). Hence, considering fragility dispersion, for a damage state where the median estimates are close, there may be relatively similar probability of the abutment seat and the column exceeding the damage state.

The seismic performances of bridges are significantly influenced by the failure mode of the bridge column and the seating length (for the seat abutment bridges). The following inferences can be obtained from the analytical results:

- At the slight damage state, the column is the critical component for the diaphragm abutment bridge with the splice-controlled column. However, the abutment in the trans-

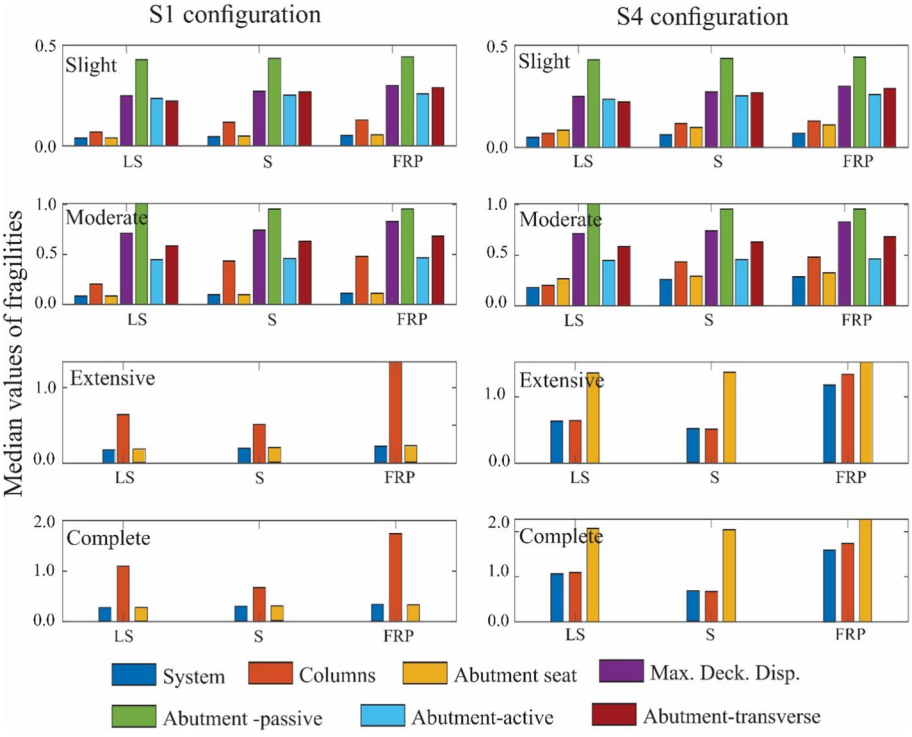

Fig. 7 Median system and component fragility estimates for S1 and S4 configurations for various damage states for the seat abutment bridges

verse is the critical component for the diaphragm abutment bridges with flexure-shear-controlled and FRP-jacketed columns. This observation is attributed to the fact that the splice-controlled columns are susceptible to initiation and propagation of vertical bond-splitting cracks at low drift demands.

- As shown in Table 5 and Fig. 7, at the slight damage state, for the seat abutment bridge, the critical component is dependent on the column failure mode and provided seating length (See Fig. 7). For small seating lengths (e.g. S1), the critical component is the abutment seat for all considered bridges. At larger seating lengths (e.g. S4), the critical component is dependent on the column failure mode. The critical component for the bridges with splice-controlled and flexure-shear-controlled columns is the column, while the critical component for the bridge with FRP-jacketed column is the abutment seat.
- As shown in Fig. 7, comparing the median fragility of the splice-controlled and flexure-shear critical columns, it is observed that the bridges with flexure-shear-controlled columns have a higher probability of exceeding the extensive and complete damage state. Further discussions are provided subsequently in this section.
- For the seat abutment bridges with FRP-jacketed columns, irrespective of the seating length, the abutment unseating is the critical component. It is concluded that in cases where only local retrofit of the column is carried out, the bridge vulnerability may switch to the abutment seat; hence, care must be taken to ensure the abutment seat fragility is desirable—else, measures should be taken to reduce the probability of abutment seat failure.

System fragility can be characterised by a lognormal distribution with median (λ) and dispersion (ζ). Table 6 outlines the median and dispersion of the system level fragilities for the selected bridge configurations. The relative vulnerability of the bridge configurations

Table 6 Selected bridge class fragilities

Bridge type	Sub-classes	Slight		Moderate		Extensive		Complete	
		λ (*g*)	ζ	λ (*g*)	ζ	λ (*g*)	ζ	λ (*g*)	ζ
Diaphragm	LS-D	0.115	0.496	0.318	0.482	0.950	0.507	1.532	0.503
	S-D	0.102	0.556	0.325	0.525	0.610	0.550	0.786	0.553
	FRP-D	0.130	0.519	0.428	0.486	1.808	0.510	2.356	0.548
Seat	LS-S-S1	0.039	0.599	0.084	0.620	0.176	0.642	0.268	0.631
	LS-S-S2	0.049	0.567	0.181	0.565	0.482	0.578	0.771	0.593
	LS-S-S3	0.051	0.587	0.182	0.566	0.600	0.567	1.000	0.572
	LS-S-S4	0.050	0.578	0.181	0.560	0.632	0.576	1.066	0.573
	S-S-S1	0.046	0.583	0.099	0.626	0.195	0.616	0.291	0.601
	S-S-S2	0.063	0.570	0.260	0.533	0.454	0.566	0.617	0.567
	S-S-S3	0.063	0.570	0.258	0.524	0.510	0.571	0.663	0.567
	S-S-S4	0.062	0.562	0.260	0.525	0.515	0.569	0.673	0.578
	FRP-S-S1	0.052	0.499	0.110	0.529	0.220	0.543	0.330	0.536
	FRP-S-S2	0.070	0.475	0.286	0.452	0.640	0.509	0.951	0.512
	FRP-S-S3	0.072	0.485	0.290	0.459	0.985	0.489	1.393	0.475
	FRP-S-S4	0.070	0.473	0.287	0.449	1.170	0.459	1.598	0.458
HAZUS	HWB20	0.350	0.600	0.450	0.600	0.550	0.600	0.800	0.600

for a specific limit state can be obtained by comparing the median values. A larger median value points to a less vulnerable bridge.

The following inferences can be drawn from Table 6:

- In general, bridges with flexure-shear-controlled columns are more vulnerable than bridges with splice-controlled columns for extensive and complete damage states. The conclusion is true for diaphragm and seat abutment bridges. This is attributed to the fact that the development of a diagonal failure plane in flexure-shear-controlled columns leads to faster degradation of lateral resistance and loss of axial load-bearing capacity. Hence, bridges with flexure-shear-controlled columns could be prioritised for retrofit over bridges with splice-controlled columns.
- The FRP retrofitting of columns can significantly enhance the performance of the bridges in the case of diaphragm abutment bridges. The relative change in the median value of fragilities of bridges with FRP-jacketed columns compared to bridges with splice-controlled columns are 13%, 35%, 90%, and 53% for the slight, moderate, extensive and complete damage, respectively. Likewise, in comparison with the bridges with flexure-shear-controlled columns, bridges with FRP-jacketed columns are 27%, 31%, 196%, and 199% less vulnerable for the slight, moderate, extensive, and complete damage states. Hence, it can be concluded that well-designed FRP retrofitting is sufficient to reduce the seismic vulnerability of bridges with diaphragm abutments constructed before the 1970s, even under large events.
- The difference in vulnerabilities for seat abutment bridges between the seating length configurations S3 and S4 is marginal, both for bridges with flexure-shear-controlled columns and bridges with splice-controlled columns. It is attributed to the fact that column vulnerability dictates the system vulnerability. Hence column jacketing is a viable solution to these configurations. However, even with retrofitting, the change in median vulnerability is less noticeable for S1 and S2 configurations. As unseating governs the failure mode in these configurations, both column jacketing and seating length increasing strategies are required for these configurations to attain a noticeable reduction in vulnerability.
- HAZUS (FEMA 2003) suggests the same fragility values for the seat and diaphragm abutment bridges (Table 6). Consistent with the previous studies (Mangalathu et al. 2017), these studies show that such a conclusion is not valid for the selected bridge configurations. Although HAZUS provide a conservative estimate (for extensive and complete damage states) in the case of diaphragm abutment bridges and seat abutment with splice-controlled columns, it significantly underestimates the fragility values for seat abutment bridges with flexure-shear-controlled columns.
- Seat abutments are more vulnerable than diaphragm abutment bridges for splice-controlled configuration. Even for seat width configurations that have a seat width of more than 24 inches, seat-abutment bridges are 130%, 75%, 50%, and 43% more vulnerable than diaphragm abutment bridges for the damage states slight, moderate, extensive, and complete damage, respectively. For bridges with flexure-shear-controlled columns, the trend is reversed: seat abutment bridges are 39%, 20%, 15%, and 14% more vulnerable than diaphragm abutment bridges. This underscores the need to account for the detailing strategies along with bridge configurations in the revision of HAZUS values for damage assessment.

8 Conclusions

Due to a lack of consideration for seismic detailing, a significant proportion of pre-1970s bridges have splice-deficient bridge columns. Past earthquake events have shown that these splice-deficient bridge columns are susceptible to shear-controlled or splice-controlled mechanisms. Experimental results have shown that the response of splice-deficient bridge columns is failure mode-dependent. From a seismic assessment and retrofit prioritisation perspective, it is important to understand the seismic fragility of as-built bridges with splice-deficient columns. Likewise, it is also relevant to understand the probable seismic performance of retrofitted bridges.

This study presents an approach for modelling the response of as-built and retrofitted bridge columns using hinge-type models. The hinge-type models are less computationally expensive than fibre-type models and can effectively capture the hysteretic response of as-built and retrofitted bridge columns. The adequacy of the hinge-type models was demonstrated using experimental data.

Using the adopted hinge-type models, fragility analysis is carried out for 15 configurations of as-built (splice-controlled and flexure-shear controlled) and retrofitted seat and diaphragm abutment bridges in California. Results showed that the seismic performances of bridges are significantly influenced by the failure mode of the bridge column and the seating length (for the seat abutment bridges). The bridge column is the critical component for the diaphragm abutment bridge with splice-controlled columns for the slight, moderate, extensive and complete damage states. However, for the diaphragm abutment bridges with flexure-shear-controlled columns and FRP-jacketed columns, the abutment in the transverse is the critical component for the slight and moderate damage states. The columns are the critical components for extensive and complete damage states of the bridges with flexure-shear controlled columns and FRP-jacketed columns. In the case of the seat abutment bridges, the critical component is dependent on the column failure mode and provided seating length. For small seating lengths, the critical component is the abutment seat. In contrast, at larger seating lengths, the critical component can be the abutment seat or column, depending on the column failure mode. In general, bridges with flexure-shear-controlled columns are more vulnerable than bridges with splice-controlled columns for extensive and complete damage states. Bridges with flexure-shear-controlled columns should be prioritised for retrofit over bridges with splice-controlled columns. It is also noted that the HAZUS fragility functions need extensive revision and should account for the probable failure mode of columns in the estimation of fragility values. As unseating governs the failure mode in some bridge configurations, both column jacketing and seating length increasing strategies are required to attain a desirable reduction in the vulnerability.

Further studies are needed to account for the material, structural and geometric uncertainties in the generation of bridge fragilities as this study does not account for these uncertainties. However, the proposed model can be extended to such studies. The effect of skew, unbalanced frames, and curvature are not considered in this study. Further studies are needed in that direction.

Funding This research received no specific grant from any funding agency in the public, commercial, or not-for-profit sectors.

Data availability The datasets generated during and/or analysed during the current study are available from the corresponding author upon reasonable request.

Declarations

Conflict of interests The authors have no relevant financial or non-financial interests to disclose.

References

Alvarez JC, Brena SF (2014) Nonlinear modeling parameters for jacketed columns used in seismic rehabilitation of RC buildings. Special Publication 297:1–22

ASCE (2017) Seismic evaluation and retrofit of existing buildings: ASCE/SEI 41–17. American Society of Civil Engineers, Reston, VA

Baker JW, Lin T, Shahi SK, Jayaram N (2011) New ground motion selection procedures and selected motions for the PEER transportation research program. Pacific Earthquake Engineering Research Center. University of California, Berkeley, CA, PEER Report

Banerjee S, Shinozuka M (2008) Mechanistic quantification of RC bridge damage states under earthquake through fragility analysis. Probab Eng Mech 23(1):12–22

Billah AHMM, Alam MS, Bhuiyan MAR (2013) Fragility analysis of retrofitted multicolumn bridge bent subjected to near-fault and far-field ground motion. J Bridge Eng Am Soc Civil Eng 18(10):992–1004

Boys A (2009) Assessment of the seismic performance of inadequately detailed reinforced concrete columns. In: Masters thesis, Department of Civil and Natural Resources Engineering, University of Canterbury

Breña SF, Schlick BM (2007) Hysteretic behavior of bridge columns with FRP-jacketed lap splices designed for moderate ductility enhancement. J Compos Constr Am Soc Civil Eng 11(6):565–574

Chai YH, Priestley MJN, Seible F (1991) Seismic retrofit of circular bridge columns for enhanced flexural performance. Struct J 88(5):572–584

Choi E (2002) Seismic Analysis and Retrofit of Mid-America Bridges. In: PhD thesis. Georgia Institute of Technology

Cornell CA, Jalayer F, Hamburger RO, Foutch DA (2002) Probabilistic basis for 2000 SAC federal emergency management agency steel moment frame guidelines. J Struct Eng Am Soc Civil Eng 128(4):526–533

Elwood KJ (2004) Modelling failures in existing reinforced concrete columns. Can J Civ Eng 31(5):846–859

FEMA (2003) HAZUS MR4 multi-hazard loss estimation methodology – earthquake model – technical manual

Fung GG, Lebeau RJ, Klein ED, Belvedere J, Goldschmidt, AF (1971) Field investigation of bridge damage in the San Fernando earthquake. Preliminary Report

Ghosh KK, Sheikh SA (2007) Seismic upgrade with carbon fiber-reinforced polymer of columns containing lap-spliced reinforcing bars. ACI Struct J Am Concr Inst 104(2):227

Harajli MH, Dagher F (2008) Seismic strengthening of bond-critical regions in rectangular reinforced concrete columns using fiber-reinforced polymer wraps. ACI Struct J 105(8):68–77

Harajli MH, Rteil AA (2004) Effect of confinement using fiber-reinforced polymer or fiber-reinforced concrete on seismic performance of gravity load-designed columns. Struct J 101(1):47–56

Haroun MA, Elsanadedy HM (2005) Fiber-reinforced plastic jackets for ductility enhancement of reinforced concrete bridge columns with poor lap-splice detailing. J Bridge Eng Am Soc Civil Eng 10(6):749–757

Haselton CB, Liel AB, Taylor-Lange SC, Deierlein GG (2016) Calibration of model to simulate response of reinforced concrete beam-columns to collapse. ACI Struct J 113(6):1141–1152

HAZUS-MH (2003) Multi-hazard loss estimation methodology: earthquake model. Washington (DC): Department of Homeland Security, FEMA

Housner GW (1994) The continuing challenge—The Northridge earthquake of January 17, 1994. Report to the Director, California Department of Transportation by the Seismic Advisory Board, California

Huo Y, Zhang J (2013) Effects of pounding and skewness on seismic responses of typical multispan highway bridges using the fragility function method. J Bridge Eng Am Soc Civil Eng 18(6):499–515

Jennings PC (1997) Enduring lessons and opportunities lost from the San Fernando earthquake of February 9, 1971. Earthq Spectra 13(1):25–44
Kim S-H, Shinozuka M (2004) Development of fragility curves of bridges retrofitted by column jacketing. Probab Eng Mech 19(1–2):105–112
LeBorgne MR, Ghannoum WM (2014) Calibrated analytical element for lateral-strength degradation of reinforced concrete columns. Eng Struct 81:35–48
Lee B (1990) Loma Prieta Earthquake Reconnaisance Report-Supplement to Earthquake Spectra v. 6. Earthq Eng Res Inst 90-01
Lew HS (1990) Performance of structures during the Loma Prieta earthquake of October 17, 1989 (NIST SP 778)
Lignos DG, Krawinkler H (2011) Deterioration modeling of steel components in support of collapse prediction of steel moment frames under earthquake loading. J Struct Eng Am Soc Civil Eng 137(11):1291–1302
Lynn AC, Moehle JP, Mahin SA, Holmes WT (1996) Seismic evaluation of existing reinforced concrete building columns. Earthq Spectra 12(4):715–739
Mackie K, Stojadinović B (2001) Probabilistic seismic demand model for California highway bridges. J Bridge Eng Am Soc Civil Eng 6(6):468–481
Mangalathu S, Jeon J-S, Padgett JE, DesRoches R (2016) ANCOVA-based grouping of bridge classes for seismic fragility assessment. Eng Struct 123:379–394
Mangalathu S, Soleimani F, Jeon J-S (2017) Bridge classes for regional seismic risk assessment: improving HAZUS models. Eng Struct 148:755–766
Mangalathu S, Choi E, Park HC, Jeon J-S (2018) Probabilistic seismic vulnerability assessment of tall horizontally curved concrete bridges in California. J Perform Constr Facil 32(6):04018080
Mangalathu S (2017) Performance based grouping and fragility analysis of box-girder bridges in California. In: PhD thesis, Georgia Institute of Technology
Massicotte B, Boucher-Proulx G (2008) Seismic retrofitting of rectangular bridge piers with UHPFRC jackets. In: BEFIB 2008: 7th RILEM international symposium on fibre reinforced concrete, RILEM Publications SARL, pp 969–975
Mazzoni S, McKenna F, Scott MH, Fenves GL (2006) OpenSees command language manual. Pacific Earthquake Engineering Research (PEER) Center, Berkeley, California, United States, p 264
Megally SH, Silva PF, Seible F (2001) Seismic response of sacrificial shear keys in bridge abutments. University of California, San Diego, Department of Structural Engineering, Structural Systems Research Project
Melek M, Wallace JW (2004) Cyclic behavior of columns with short lap splices. ACI Struct J 101(6):802–811
Muthukumar S, DesRoches R (2006) A Hertz contact model with nonlinear damping for pounding simulation. Earthq Eng Struct Dyn 35(7):811–828
Nielson BG, DesRoches R (2007) Seismic fragility methodology for highway bridges using a component level approach. Earthq Eng Struct Dyn 36(6):823–839
Nims DK, Miranda E, Aiken ID, Whittaker AS, Bertero VV (1989) Collapse of the cypress street viaduct as a result of the Loma Prieta Earthquake: Berkeley, University of California. Earthquake Engineering Research Center Report, p 85
Opabola EA, Elwood KJ (2020) Simplified approaches for estimating yield rotation of reinforced concrete beam-column components. ACI Struct J 117(4):279–291
Opabola EA, Elwood KJ (2021) Seismic assessment of reinforced concrete columns with short lap splices. Earthq Spectra. https://doi.org/10.1177/8755293021994834
Opabola EA, Elwood KJ, Liel AB (2021) Evaluation of seismic performance of as-built and retrofitted reinforced concrete frame structures with LAP splice deficiencies. (January), pp 1–22
Padgett JE, DesRoches R (2008) Methodology for the development of analytical fragility curves for retrofitted bridges. Earthq Eng Struct Dyn 37(8):1157–1174
Ramanathan KN (2012) Next generation seismic fragility curves for California bridges incorporating the evolution in seismic design philosophy. In: PhD thesis, Georgia Institute of Technology
Seible F, Priestley MJN (1999) Lessons learned from bridge performance during Northridge earthquake. Spec Publ 187:29–56
Seible F, Priestley MJN, Hegemier GA, Innamorato D (1997) Seismic retrofit of RC Columns with continuous carbon fiber jackets. J Compos Constr 1(2):52–62
Sezen H, Moehle JP (2004) Shear Strength Model for Lightly Reinforced Concrete Columns. J Struct Eng 130(11):1692–1703
Shafieezadeh A, Ramanathan K, Padgett JE, DesRoches R (2012) Fractional order intensity measures for probabilistic seismic demand modeling applied to highway bridges. Earthq Eng Struct Dyn 41(3):391–409
Shamsabadi A, Yan L (2008) Closed-form force-displacement backbone curves for bridge abutment-backfill systems. Geotech Earthq Eng Soil Dyn IV:1–10

Shinozuka M, Kim S-H, Kushiyama S, Yi J-H (2002) Fragility curves of concrete bridges retrofitted by column jacketing. Earthq Eng Eng Vib 1(2):195–205

Stefanidou SP, Kappos AJ (2021) Fragility-informed selection of bridge retrofit scheme based on performance criteria. Eng Struct 234:111976

Stefanidou SP, Paraskevopoulos EA, Papanikolaou VK, Kappos AJ (2022) An online platform for bridge-specific fragility analysis of as-built and retrofitted bridges. Bull Earthq Eng 20(3):1717–1737

Xie Y, Zhang J, DesRoches R, Padgett JE (2019) Seismic fragilities of single-column highway bridges with rocking column-footing. Earthq Eng Struct Dyn 48(7):843–864

Zhang Y, DesRoches R, Tien I (2019) Impact of corrosion on risk assessment of shear-critical and short lap-spliced bridges. Eng Struct 189(February):260–271